0026-895X/07/7205-1181–1190$20.00
MOLECULAR PHARMACOLOGY
Vol. 72, No. 5
36368/3270342
Mol Pharmacol 72:1181–1190, 2007
Printed in U.S.A.

Dimerization Region of Soluble Guanylate Cyclase Characterized by Bimolecular Fluorescence Complementation in Vivo

Christiane Rothkegel, Peter M. Schmidt, Derek-John Atkins, Linda Sarah Hoffmann, Harald H. H. W. Schmidt, Henning Schröder, and Johannes-Peter Stasch

Cardiovascular Research, Bayer HealthCare, Wuppertal, Germany (C.R., D.-J.A., L.S.H., J.P.S.); Martin-Luther-University, School of Pharmacy, Halle, Germany (C.R., L.S.H., H.S., J.P.S.); Department of Pharmacology, Monash University, Melbourne, Clayton, Victoria, Australia (P.M.S., H.H.H.W.S.); Department of Pharmaceutics, College of Pharmacy, University of Minnesota, Minneapolis, Minnesota (H.S.); and Helios Klinikum, Institute for Pathology, Wuppertal, Germany (D.-J.A.)

Received March 26, 2007; accepted August 9, 2007

ABSTRACT

The ubiquitously expressed nitric oxide (NO) receptor soluble guanylate cyclase (sGC) plays a key role in signal transduction. Binding of NO to the N-terminal prosthetic heme moiety of sGC results in ~200-fold activation of the enzyme and an increased conversion of GTP into the second messenger cGMP. sGC exists as a heterodimer the dimerization of which is mediated mainly by the central region of the enzyme. In the present work, we constructed deletion mutants within the predicted dimerization region of the sGC α_1- and β_1-subunit to precisely map the sequence segments crucial for subunit dimerization. To track mutation-induced alterations of sGC dimerization, we used a bimolecular fluorescence complementation approach that allows visualizing sGC heterodimerization in a noninvasive manner in living cells. Our study suggests that segments spanning amino acids $\alpha_1$363–372, $\alpha_1$403–422, $\alpha_1$440–459, $\beta_1$212–222, $\beta_1$304–333, $\beta_1$344–363, and $\beta_1$381–400 within the predicted dimerization region are involved in the process of heterodimerization and therefore in the expression of functional sGC.

sGC is the ubiquitously expressed intracellular receptor for the gaseous biological messenger NO. The enzyme is activated upon binding of its endogenous activator NO to its heme moiety, resulting in a strongly increased conversion of GTP to cGMP. This second messenger regulates various effector systems, such as phosphodiesterases, ion channels, and protein kinases. Thus, the NO/sGC/cGMP pathway modulates a broad range of physiological processes, including vasodilation, neurotransmission, and platelet aggregation (Hobbs, 2002; Bender and Beavo, 2006; Feil and Kemp-Harper, 2006). Because of its ubiquitous nature, the pathogenesis of various disease states, especially of the cardiovascular system, has been linked to aberrant activation of the NO/sGC/cGMP pathway (Hobbs, 2002; Feil and Kemp-Harper, 2006; Gladwin, 2006; Stasch et al., 2006)

P.M.S. is the recipient of an Alexander-von-Humboldt Lynen fellowship.
Article, publication date, and citation information can be found at http://molpharm.aspetjournals.org.
doi:10.1124/mol.107.036368.

sGC is a heterodimer consisting of an α-subunit and a heme-containing β-subunit. Although two isoforms of each subunit (α_1, α_2, β_1, and β_2) exist, only the ubiquitously expressed α_1/β_1-hetereodimer and the α_2/β_1-heterodimer, which is most abundant in brain, uterus and placenta, have been characterized as functional enzymes (Harteneck et al., 1991; Russwurm et al., 1998; Zabel et al., 1998; Hoenicka et al., 1999; Mergia et al., 2003). Because the crystal structure of sGC has not been resolved yet, most of the knowledge of the enzyme's spatial structure is based on homology to other crystallized proteins, in silico structure predictions, and biochemical approaches such as mutagenesis, enzymatic assays, or coimmunoprecipitations. Based on these results, the sGC subunits have been divided into distinct regions: the N-terminal NO-sensing heme domain (H-NOX), the central region consisting of a PER/ARNT/SIM (periodicity/aryl hydrocarbon receptor nuclear translocator/simple-minded)-like domain and an amphipathic α-helix region, and the C-terminal highly conserved catalytic domain (Gerzer et al., 1981;

ABBREVIATIONS: sGC, soluble guanylate cyclase; H-NOX, N-terminal NO-sensing heme domain; BiFC, bimolecular fluorescence complementation; BAY 58-2667, 4-[((4-carboxybutyl){2-[(4-phenethyl-benzyl)oxy]-phenethyl}amino)methyl[benzoic]acid; BAY 41-2272, 5-cyclopropyl-2-[1-(2-fluoro-benzyl)-1*H*-pyrazolo[3,4-*b*]pyridin-3-yl]-pyrimidin-4-ylamine; DEA/NO, 2-(*N*,*N*-diethylamino)-diazenolate-2-oxide; ODQ, 1*H*-(1,2,4)-oxadiazole-(4,3-*a*)-quinoxalin-1-one; YFP, yellow fluorescent protein; YC, C-terminal fragment of YFP; YN, N-terminal fragment of YFP; WT, wild-type; NBS, N-terminal binding site; CBS, C-terminal binding site.

Nioche et al., 2004; Pellicena et al., 2004; Cary et al., 2006). The β-H-NOX domain contains the prosthetic heme group, which is coordinated to this domain via the axial ligand His^{105} and the recently identified heme-binding motif Tyr^{135}, Ser^{137}, and Arg^{139} (Y-x-S-x-R) (Wedel et al., 1994; Zhao et al., 1998; Pellicena et al., 2004; Schmidt et al., 2004, 2005). Dimerization of the α/β-subunits has been proposed to be mediated mainly by the central region of sGC based on the homology of amino acids $\beta_1$340–385 to the sequence mediating particulate guanylate cyclase homodimerization and studies that identified segments spanning amino acids $\alpha_1$61–128, $\alpha_1$367–462, $\alpha_1$421–454, $\beta_1$204–244, and $\beta_1$379–408 to be responsible for subunit dimerization (Wilson and Chinkers, 1995; Zhao and Marletta, 1997; Nighorn et al., 1999; Zhou et al., 2004; Shiga and Suzuki, 2005; Wagner et al., 2005).

To further narrow the published and to identify novel amino acid segments involved in sGC heterodimerization, we identified conserved parts of the central domain of sGC via multisequence alignments and systematically deleted these residues. The impact of these alterations on the formation of functional sGC was determined by BiFC, which enabled us to visualize sGC heterodimerization in a noninvasive manner in living cells. In parallel, we investigated the activation profile of the generated mutants by using a unique cGMP reporter cell line. This cell line in combination with NO- and heme-independent sGC activators, such as BAY 58-2667, and NO-independent but heme-dependent sGC stimulators, such as BAY 41-2272, enabled us to characterize the activation profile of sGC and sGC variants directly within their cellular environment (Stasch et al., 2001; Schmidt et al., 2005; Wunder et al., 2005; Evgenov et al., 2006; Rothkegel et al., 2006).

Materials and Methods

Reagents. BAY 58-2667 and BAY 41-2272 were synthesized as described previously (Alonso-Alija et al., 2001; Straub et al., 2001). 2-(*N*,*N*-Diethylamino)-diazenolate-2-oxide (DEA/NO) and 1*H*-(1,2,4)-oxadiazole-(4,3-*a*)-quinoxalin-1-one (ODQ) were purchased from Alexis Biochemicals (San Diego, CA). All other chemicals of analytical grade were obtained from Sigma (Taufkirchen, Germany).

Construction of Fusion Proteins for BiFC Analysis. The plasmids pBiFC-YN154 and pBiFC-YC155 were kindly provided by Dr. T. Kerppola (University of Michigan, Ann Arbor, MI) and encoded amino acids 1 to 154 (YN) and 155 to 238 (YC) of enhanced YFP (Hu et al., 2002). The sequences encoding YN and YC are preceded by the linker sequences RPACKIPNDLKQKVMNH and RSIAT, respectively. To construct proteins fused to either the N terminus (YNV, YCV) or the C terminus (YNH, YCH) of sGC, sequences encoding the rat α_1- or β_1-subunit were cloned into pBiFC-YN154 and pBiFC-YC155. Sequences encoding α_1-sGC and β_1-sGC were amplified by PCR from pcDNAI/Amp and pRNAI/Amp. Primers listed in Table 1 introduced a BsiWI site and a ClaI site in pcDNA/Amp, pRNAI/Amp, pBiFC-YN154, and pBiFC-YC155. The α_1-sGC and β_1-sGC PCR products were digested with BsiWI and ClaI (Roche, Basel, Switzerland) and inserted into the pBiFC-YN154 and pBiFC-YC155 plasmids digested with the same enzymes to produce the N-terminal fused chimeras α_1-YNV, α_1-YCV, β_1-YNV, and β_1-YCV and the C-terminal fused chimeras α_1-YNH, α_1-YCH, β_1-YNH, and β_1-YCH, respectively. The integrity of all clones was verified by sequence analysis (Invitek, Berlin, Germany).

Cell Culture and Transient Transfection. The transient cotransfection of α_1- and β_1-subunits was based on a method described previously (Schmidt et al., 2005; Rothkegel et al., 2006). In brief, for cGMP readout, cGMP reporter cells were seeded on 96-well microtiter plates at a density of 10,000 cells per well. For confocal microscopy, cGMP reporter cells were seeded in eight-well glass chambers (Nalge Nunc International, Rochester, NY) at a density of 2×10^4 cells per chamber. Cells were cultured for 1 day at 37°C in a 5% CO_2 atmosphere and then cotransfected with a transfection mixture containing 36 ng of α_1-plasmid and 36 ng of β_1-plasmid, 0.12 μl of Plus reagent and 0.6 μl of LipofectAMINE (Invitrogen, Carlsbad, CA) in 100 μl of Opti-MEM serum-free medium (Invitrogen) or 250 ng of α_1-plasmid and 250 ng of β_1-plasmid, 0.84 μl of Plus reagent, and 4.2 μl of LipofectAMINE (Invitrogen) in 200 μl of Opti-MEM serum-free medium, respectively. After 3 h, the serum-free medium was exchanged for serum-containing medium, and cells were incubated for 24 h at 37°C, 5% CO_2 to ensure optimal protein expression.

cGMP Readout. The generation of the cGMP reporter cell and the cGMP readout has been described previously (Schmidt et al., 2005; Wunder et al., 2005; Rothkegel et al., 2006). In brief, for the determination of the sGC activation profile, transiently transfected cGMP reporter cells were incubated with various concentrations of the sGC stimulator BAY 41-2272 or the sGC activator BAY 58-2667 alone or in presence of DEA/NO or ODQ for 15 min at 37°C, 5% CO_2. 3-Isobutyl-1-methylxanthine (0.2 mM) was used to prevent cGMP degradation by endogenous phosphodiesterases. The biolumines-

TABLE 1
Primers used to introduce BsiWI and ClaI restriction sites in pcDNA/Amp-α_1, pRNAI/Amp-β_1, pBiFC-YN154, and pBiFC-YC155 to generate YFP-sGC fusion proteins

Plasmid	Primer	Vector
YCV		pHA/CMV (Clontech)
BsiWI site	5′-GCCATGGAGGCCGTACGTCGGGTCGTG-3′	
ClaI Site	5′-GTCGGGGTCGTGATCGATCCATCGGTCGTC-3′	
YCH		pHA/CMV (Clontech)
BsiWI site	5′-GCTGTACAAGTACGTACGCGCGGGGATCC-3′	
ClaI Site	5′-GACATGATAAGATCGATTGATGAGTTTGGAC-3′	
YNV		pFlag/CMV-2 (Sigma)
BsiWI site	5′-CTTGTCCCCCATCGTACGGGAGTCTCAGGAG-3′	
ClaI Site	5′-GCATGAGAAATCGATTCGCTGCCTC-3′	
YNH		pFlag/CMV-2 (Sigma)
BsiWI site	5′-CTATATCATGGCCGTACGATCCCGGGTGGC-3′	
ClaI Site	5′-GTGACCCCTCCCCAATCGATCTCCTGGC-3′	
α_1-sGC		pcDNAI/Amp (Invitrogen)
BsiWI site	5′-CCACTGCAAAGCGTACGGAACACCATG-3′	
ClaI Site	5′-CATCAGGGGTAGATCGATGAGCCGCATG-3′	
β_1-sGC		pRNAI/Amp (Invitrogen)
BsiWI site	5′-CAGGCTCCGGGCGTACGGTACACCATG-3′	
ClaI Site	5′-CAGGATGAAAATCGATTGGCAGCC-3′	

cence readout was initiated by application of 10 mM $CaCl_2$-containing buffer and was shown to correlate directly with the intracellular cGMP concentration as described elsewhere (Wunder et al., 2005).

BiFC Analysis by Confocal Microscopy. For analysis of individual cells by confocal microscopy, the transiently transfected cGMP reporter cells grown in eight-well glass chambers were examined with a Zeiss Confocal Microscope LSM 510 (Carl Zeiss, Jena, Germany) using an oil Plan 63× objective (Carl Zeiss, Jena, Germany). YFP was excited at 514 nm and detected at 530 to 600 nm. Images were taken with an integrated charge-coupled device camera, processed, and analyzed with the LSM Image software (Carl Zeiss). To adjust size and contrast, the images were further processed with Photoshop software (Adobe Systems, München, Germany).

Western Blotting. To validate the transient expression of sGC in the cGMP reporter cell line, cells were transfected as described above. After 24 h, cells were lysed and centrifuged at 100,000*g*. Proteins of the supernatant (10 μg) were separated on a 10% polyacrylamide gel (Anamed, Darmstadt, Germany) by electrophoresis as described previously (Rothkegel et al., 2006). The protein bands were transferred to a nitrocellulose membrane (Mini-PROTEAN II cell; Trans-Blot Transfer Medium Pure Nitrocellulose Membrane; 0.2 μM, Bio-Rad Laboratories, München, Germany). The individual sGC subunits were detected using polyclonal antibodies directed against epitopes of the α_1-sGC and the β_1-sGC subunits (Cayman Chemical, Tallin, Estonia). Actin was used as a loading control and detected by a monoclonal anti-β-actin antibody (Sigma). Detection was performed by enhanced chemiluminescence method (Becker et al., 1999).

Mutagenesis. The mutagenesis was performed using the QuikChange-XL site-directed mutagenesis kit (Stratagene, La Jolla, CA) according to manufacturer's instructions. Primers listed in Table 2 were used to generate the deletion mutants screened by BiFC analysis and in the cGMP readout system. The accuracy of the mutations was verified by sequencing (Invitek, Berlin, Germany).

Results

Generation of Functional Fluorescent α_1/β_1-sGC. The recently developed BiFC approach was applied to visualize the heterodimerization of α_1-sGC and β_1-sGC subunits (Hu et al., 2002). In general, this approach is based on the complementation of a fluorophore such as YFP from two nonfluorescent fragments upon interaction of the two proteins fused to each fragment (Kerppola, 2006a,b).

To construct a fluorescent α_1/β_1-sGC heterodimer, we fused the N-terminal YFP fragment (YN) and the C-terminal fragment (YC) to the N terminus (YNV, YCV) and the C terminus (YNH, YCH) of the α_1- and β_1-subunit, respectively (Fig. 1 A). The generated fusion proteins were transiently expressed in a cGMP reporter cell line based on a Chinese hamster ovary cell line stably transfected with the cyclic nucleotide gated olfactory CNG2A-channel and cytosolic aequorin (Wunder et al., 2005). Fluorescence was detected by confocal microscopy, and enzyme activity was measured as luminescence, indicated in relative light units, which was shown to correlate with the intracellular cGMP concentration (Wunder et al., 2005). Coexpression of α_1-YCH/β_1-YNH-sGC and α_1-YNV/β_1-YCV-sGC resulted in a fluorescence signal located in the cytosol (Fig. 1, C and D). Other possible combinations of both complementary YFP fragments did not lead to any detectable fluorescence signal, indicating that functional YFP complementation was not achieved (Fig. 1A). YN-YC-sGC fusion constructs that showed fluorescence complementation were expressed at similar levels (Fig. 1E). To exclude the possibility that the fused YN/YC fragments affect the enzyme's catalytic activity, the activation profile of α_1-YCH/β_1-YNH-sGC and α_1-YNV/β_1-YCV-sGC was characterized in the cGMP reporter cell and compared with wild-type (WT) sGC.

Cotransfection of cGMP reporter cells with WT-α_1-sGC and WT-β_1-sGC cDNA resulted in an activation profile characteristic for the native, heme-containing enzyme. The NO-independent but heme-dependent sGC stimulator BAY 41-2272 stimulated the enzyme in a concentration-dependent manner with an EC_{50} value of 467 ± 13.9 nM. In the presence of 10 nM DEA/NO, which caused a 4.3-fold stimulation, the concentration response curve was shifted to the left as reflected by the determined EC_{50} value of 205 ± 12.8 nM (Figs. 2A and 3). The NO- and heme-independent sGC activator BAY 58-2667 induced a 15-fold stimulation (EC_{50} 69 ± 9.6 nM) of enzyme activity, which was further increased up to 30-fold

TABLE 2
Primers used to generate deletion mutants within the proposed dimerization domains of both sGC subunits as described under *Materials and Methods*

Mutation	Primer
α_1 (Δ283–292)-YNV	5′-CTAGTGATCCCTACTTCGCTCCTGGACCGTGACCTGGCCATTC-3′
α_1 (Δ363–372)-YNV	5′-GTGAAGAAATCTTCAAGGGTTGTTGAATCCAGTGCCATCTTGTTC-3′
α_1 (Δ373–382)-YNV	5′-TCAAAGGTCAAATGATCTACATCTCGCCGTGTGTGGACAGATTGG-3′
α_1 (Δ383–392)-YNV	5′-GTGCCATCTTGTTCTTAGGGACAGGACGGGGTCTCTATCTG-3′
α_1 (Δ393–402)-YNV	5′-GTGGACAGATTGGAAGATTTCCCGATTCATAATGCCCTGAGG-3′
α_1 (Δ403–412)-YNV	5′-CGGGGTCTCTATCTGTCTGACATCTTGATAGGGGAACAGGCACGG-3′
α_1 (Δ413–422)-YNV	5′-CATAATGCCCTGAGGGATGTTGTCGGCCTCAAGAAGAGGTTGGG-3′
α_1 (Δ440–449)-YNV	5′-CCTTGGAGCATGCCCACCAAGTAGATCTCCTGTGTTCTATC-3′
α_1 (Δ450–459)-YNV	5′-GAGGAGGAGAAGAAGAAGACGGAGGTTGCTCAGCAGCTCTGGC-3′
α_1 (Δ460–469)-YNV	5′-CTGTGTTCTATCTTTCCCTCTATTGTGCAAGCCAAGAAGTTC-3′
α_1 (Δ470–479)-YNV	5′-CAGCAGCTCTGGCAAGGACAAACCATGCTCTTCTCAGATATC-3′
β1 (Δ212–222)-YCV	5′-GACTCCCGTATCAGCCCGTACATATTTGACCGGGACCTAGTAG-3′
β1 (Δ304–313)-YCV	5′-CTGGGGCAGAGATTAGCTGCCCGGAAGCAGATAGCATCCTC-3′
β1 (Δ314–323)-YCV	5′-CAAAGGCCAAATGATCTATTTATCACCAAGTGTGATGAACTTG-3′
β1 (Δ324–333)-YCV	5′-GATAGCATCCTCTTCCTCTGTACAAGAAGAGGCCTGTACCTG-3′
β1 (Δ334–343)-YCV	5′-GTGATGAACTTGGATGACCTACCTCTCCATGATGCTACACGAG-3′
β1 (Δ344–353)-YCV	5′-GAGGCCTGTACCTGAGTGACATCCTTTTGGGAGAACAGTTCCGG-3′
β1 (Δ354–363)-YCV	5′-GATGCTACACGAGACCTGGTCAACTGACACAAGAGCTGGAAATC-3′
β1 (Δ381–390)-YCV	5′-CAGGCTGCAGCTCACACTGGACACATTGCTATATTCTGTTC-3′
β1 (Δ391–400)-YCV	5′-GAGGATGAGAAGAAAAAGACATCTGTTGCCAATGAGCTGAGAC-3′
β1 (Δ401–410)-YCV	5′-CTATATTCTGTTCTCCCTCCACCAGTGCCGGCCAAAAGATAC-3′
β1 (Δ411–420)-YCV	5′-CAATGAGCTGAGACACAAGCGTACCATCCTCTTCAGTGGCATTGTG-3′

(EC_{50} 30 ± 6.6 nM) in the presence of ODQ (Fig. 2B). Thus, the activation profile of the cGMP cells transiently transfected with the native enzyme was similar to that observed for isolated sGC.

In contrast to the WT enzyme, the α_1-YCH/β_1-YNH-sGC was unresponsive to BAY 41-2272 or BAY 58-2667 alone or combined with DEA/NO or ODQ, respectively, indicating that fusion of the YN/YC-fragments to the sGC catalytic domain disturbed the cGMP-forming capability of the enzyme (Figs. 2, C and D, and 3).

Fusion of the YFP fragments to the N termini of the α- and β-subunits of sGC caused only slight alterations of the enzyme's catalytic activity. Coexpression of α_1-YNV/β_1-YCV-sGC resulted in an activation profile similar to the native, heme-containing enzyme. BAY 41-2272 stimulated the α_1-YNV/β_1-YCV-sGC concentration-dependently with an EC_{50} value of 540 ± 19.5 nM and addition of 10 nM DEA/NO, which stimulated the α_1-YNV/β_1-YCV-sGC to a maximum of 4.86-fold, caused a potentiation of the BAY 41-2272-induced stimulation, reducing the EC_{50} value to 430 ± 17.5 nM (Figs. 2E and 3). BAY 58-2667 induced a concentration-dependent activation with an EC_{50} value of 15 ± 0.96 nM that was decreased in the presence of ODQ to 3.9 ± 0.66 nM (Fig. 2F). Because the C-terminal sGC-BiFC fusion constructs were nonfunctional, all subsequent experiments were performed with the N-terminal α_1-YNV/β_1-YCV construct.

Characterization of the α_1-sGC and β_1-sGC Deletion Mutants. Conserved segments within the predicted dimerization regions of α_1-sGC and β_1-sGC were identified by a multiple sequence alignment (Fig. 4, red residues). The identified amino acids were deleted, and the various constructs were transiently transfected into the cGMP reporter cell for protein expression. The ability of the deletion mutants to heterodimerize was characterized by BiFC, and the activation profile was characterized by luminescence as described above.

Coexpression of the α_1-YNV deletion mutants α_1(Δ283–292), α_1(Δ373–382), α_1(Δ383–392), α_1(Δ393–402), α_1(Δ460–

A

	Fluorescence signal
Untransfected control	n.d.[a]
α_1/β_1-sGC	n.d.
α_1-YCV/β_1-YNV-sGC	n.d.
α_1-YCH/β_1-YNH-sGC	+
α_1-YNV/β_1-YCV-sGC	+
α_1-YNH/β_1-YCH-sGC	n.d.
α_1-YCV/β_1-YNH-sGC	n.d.
α_1-YCH/β_1-YNV-sGC	n.d.
α_1-YNV/β_1-YCH-sGC	n.d.
α_1-YNH/β_1-YCV-sGC	n.d.
α_1-YCH/α_1-YNV-sGC	n.d.
α_1-YCH/α_1-YNH-sGC	n.d.
α_1-YNV/α_1-YCV-sGC	n.d.
α_1-YNV/α_1-YCH-sGC	n.d.
β_1-YCV/β_1-YNV-sGC	n.d.
β_1-YCV/β_1-YNH-sGC	n.d.
β_1-YNH/β_1-YCV-sGC	n.d.
β_1-YNH/β_1-YCH-sGC	n.d.

[a]n.d., not detectable

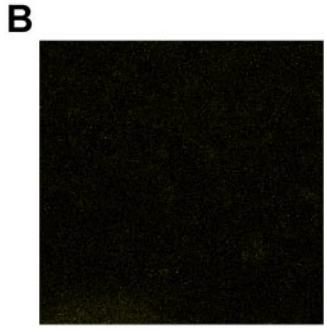

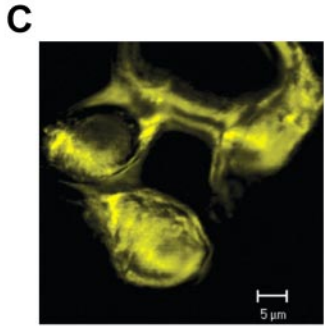

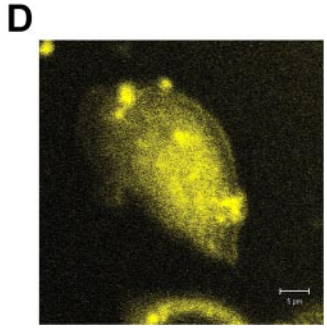

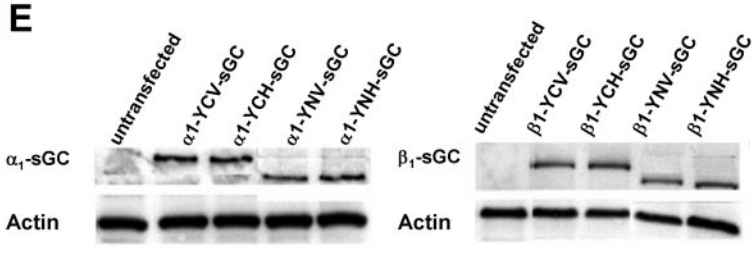

Fig. 1. Construction and validation of BiFC constructs. A, fluorescence signals of YFP fragments (YN, YC) fused either at the N terminus of sGC α_1- and β_1-subunits (α_1-YNV, α_1-YCV, β_1-YNV, β_1-YCV) or at the C terminus of α_1- or β_1-sGC (α_1-YNH, α_1-YCH, β_1-YNH, β_1-YCH). Imaging was performed by confocal microscopy of transiently transfected cGMP reporter cells. Fluorescence signal of representative, transiently transfected cGMP reporter cells transfected with α_1/β_1-sGC (B), α_1-YCH/β_1-YNH-sGC (C) and α_1-YNV/β_1-YCV-sGC (D). E, Western blots of the cytosolic fractions of control and cGMP reporter cells transiently transfected with the indicated constructs. Both enzyme subunits were detected by using polyclonal antibodies as described under *Materials and Methods*.

469), and α_1(Δ470–479) with WT-β_1-YCV as well as the β_1-YCV deletion mutants β_1(Δ334–343), β_1(Δ401–410), and β_1(Δ411–420) with WT-α_1-YNV-sGC resulted in a fluorescence signal similar to that of the fluorophore-tagged WT enzyme. The observed fluorescence indicates functional heterodimerization of both sGC subunits in the cytosol of the cell (Fig. 5A). α_1(Δ393–402), β_1(Δ334–343), and β_1(Δ411–420) were mainly localized in focal areas and not in the entire cytosolic department (Fig. 5A). Coexpression of all other deletion mutants resulted in no detectable fluorescence, suggesting a putative involvement of the deleted residues in the process of sGC heterodimerization (Fig. 4, Supplemental Data). To exclude the possibility that this loss of fluorescence was due to impaired expression or decreased protein stability, expression levels of the transiently transfected deletion mutants were determined by Western blot analysis. As shown in Fig. 5B, all constructs were expressed at a similar level, suggesting that the observed lack of fluorescence was due to the inability to form functional sGC α_1/β_1-heterodimers.

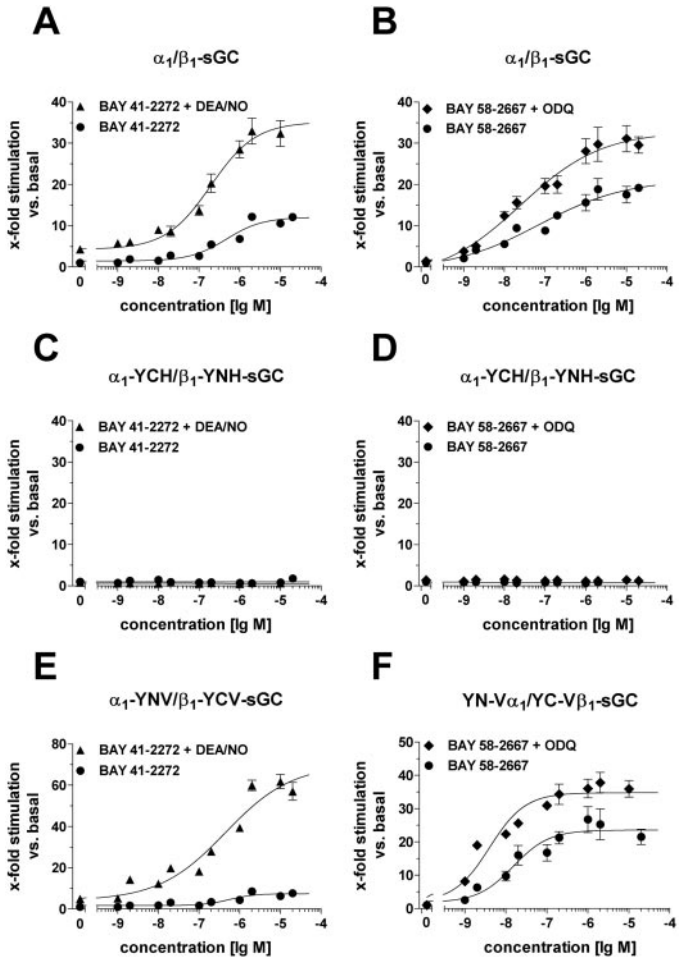

Fig. 2. Activation profile of α_1/β_1-sGC and α_1/β_1-sGC-YFP fusion proteins. Activation pattern of WT-sGC (A and B), α_1-YCH/β_1-YNH-sGC (C and D), and α_1-YNV/β_1-YCV-sGC (E and F) incubated with increasing concentrations of BAY 41-2272 or BAY 58-2667 alone or in the presence of a fixed concentration DEA/NO (10 nM) or ODQ (10 μM), respectively. cGMP reporter cells were transiently cotransfected with the indicated α_1- and β_1-subunit of sGC. Enzyme activation is represented as -fold compared with the transfected but not stimulated control. Data are shown as mean ± S.E.M. from three to five independent experiments performed in quadruplicate.

Deletion of segments 283–292, 373–382, 383–392, and 393–402 of the α_1-YNV-sGC and 334–343 of β_1-YCV-sGC resulted in the expression of a functionally active enzyme (Fig. 6, A–J). The sGC stimulator BAY 41-2272 stimulated α_1(Δ283–292)/β_1-sGC by ≤25-fold. This activation was potentiated in the presence of DEA/NO ≤150-fold (Fig. 6A). In the case of α_1(Δ373–382)/β_1-sGC, BAY 41-2272 induced a concentration dependent enzyme stimulation of ≤90-fold that was potentiated up to 200-fold upon combination with DEA/NO (Fig. 6C). The α_1(Δ383–392)/β_1-sGC was stimulated by BAY 41-2272 concentration-dependently to ≤3-fold and addition of DEA/NO potentiated the BAY 41-2272 induced enzyme activation ≤10-fold (Fig. 6E). α_1(Δ393–402)/β_1-sGC and α_1/β_1(Δ334–343)-sGC were only responsive to a combination of BAY 41-2272 and DEA/NO ≤25- and ≤12-fold, respectively (Fig. 6, G and I). The heme-independent sGC activator BAY 58-2667 induced a concentration dependent activation of α_1(Δ283–292)/β_1-sGC to a maximum of 60-fold (Fig. 6B). The α_1(Δ373–382)/β_1-sGC was activated by BAY 58-2667 ≤20-fold, and the α_1(Δ383–392)/β_1-sGC was activated ≤130-fold (Fig. 6, D and F). In the case of α_1(Δ393–402)/β_1-sGC and α_1/β_1(Δ334–343)-sGC, BAY 58-2667 activated the altered enzymes to a maximum of 5- and 2-fold, respectively (Fig. 6, H and J). The BAY 58-2667-induced enzyme activation was potentiated in the presence of ODQ for α_1(Δ373–382)/β_1-sGC only (Fig. 6D). All other deletion mutants were unresponsive to BAY 41-2272, BAY 58-2667 alone, or in combination with DEA/NO or ODQ (see Supplemental Data).

Discussion

Protein dimerization frequently leads to changes in ligand affinity and changes in the localization and/or alteration of the enzymatic capacity (Luttrell, 2006). The ubiquitous NO receptor sGC must undergo heterodimerization to obtain catalytic activity (Harteneck et al., 1991; Zabel et al., 1998; Hoenicka et al., 1999; Feil and Kemp-Harper, 2006).

The structural basis of sGC heterodimerization is still poorly understood. A decade ago, the amino acid region $\beta_1$340–385 upstream of the enzyme's catalytic domain was postulated to play a key role in heterodimer formation of sGC. This assumption was based on homologies to the respective sequence mediating dimerization of the membrane

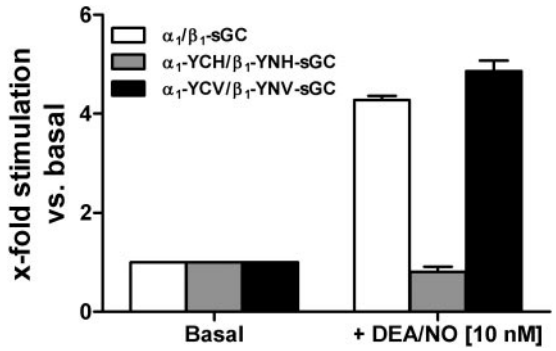

Fig. 3. Activation of α_1/β_1-sGC and α_1/β_1-sGC-YFP fusion proteins by DEA/NO. Activation of WT-sGC (white bar), α_1-YCH/β_1-YNH-sGC (gray bar), and α_1-YNV/β_1-YCV-sGC (black bar) alone or incubated with DEA/NO (10 nM). cGMP reporter cells were transiently cotransfected with the indicated α_1- and β_1-subunit of sGC. Enzyme activation is represented as -fold compared with the transfected but not stimulated control. Data are shown as mean ± S.E.M. from three to five independent experiments performed in quadruplicate.

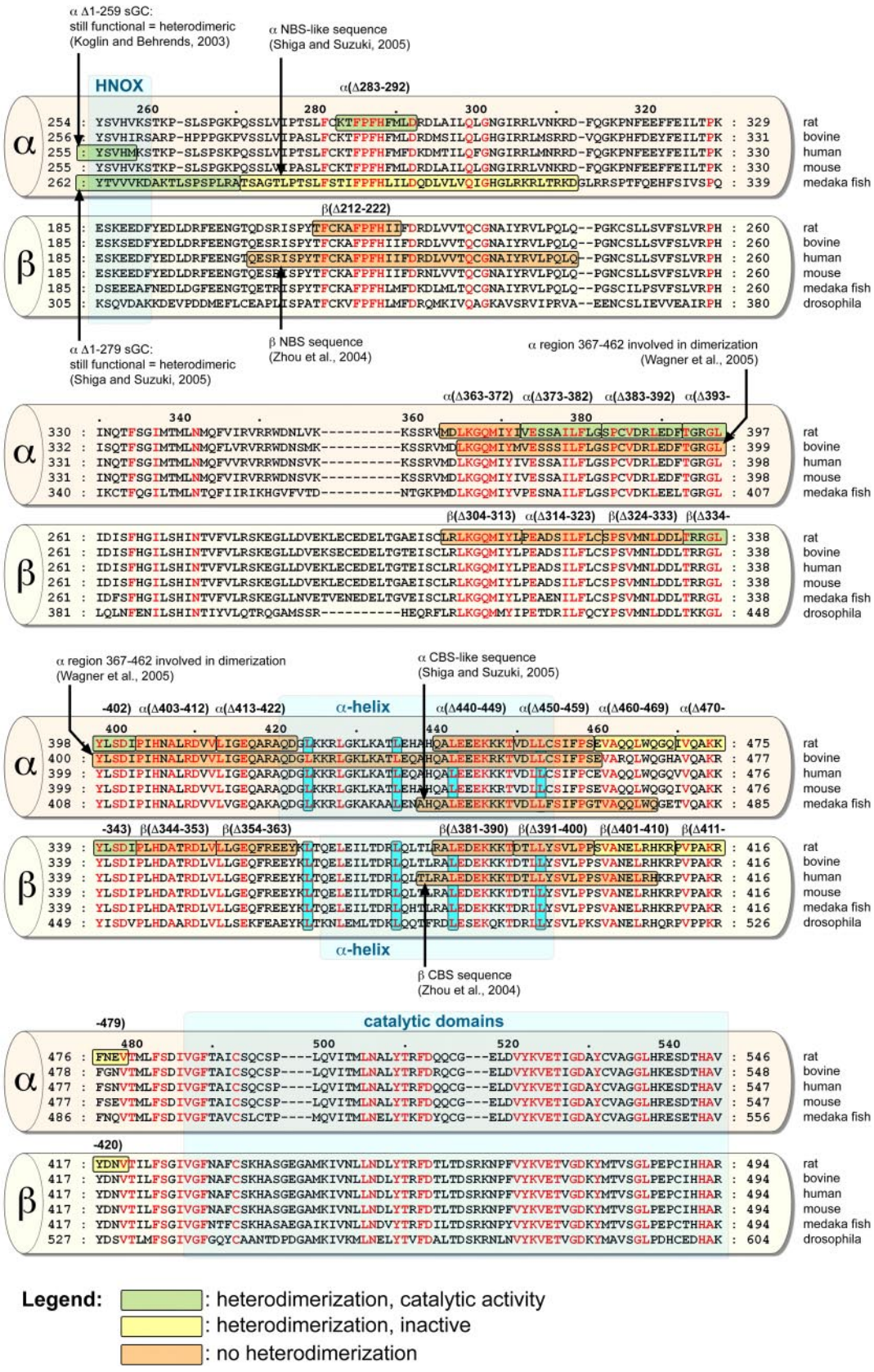

Fig. 4. Overview of identified dimerization regions of α_1/β_1-sGC. Multisequence alignment of sGC α and β subunits from the following species (UniProtKB/Swiss-Prot accession numbers in parentheses): rat α_1 (P19686), bovine α_1 (P19687), human α_1 (Q02108), mouse α_1 (Q9ERL9), medaka fish α_1 (P79997), rat β_1 (P20595), bovine β_1 (P16068), human β_1 (Q02153), mouse β_1 (O54865), medaka fish β_1 (P79998), and *Drosophila melanogaster* β_1 (Q24086). Conserved residues are red. The start and end points of the H-NOX and catalytic domains, respectively, are blue. sGC α_1/β_1 interaction sites reported in the present work or by others are highlighted as follows: amino acid regions contributing to α_1/β_1-sGC dimerization are orange. Segments that are not involved in subunit dimerization but seem to be critical for functional enzyme activity are yellow. Regions analyzed and identified to be neither involved in α_1/β_1-sGC dimerization nor critical for sGC activity are green. The conserved leucines mentioned in the text are blue.

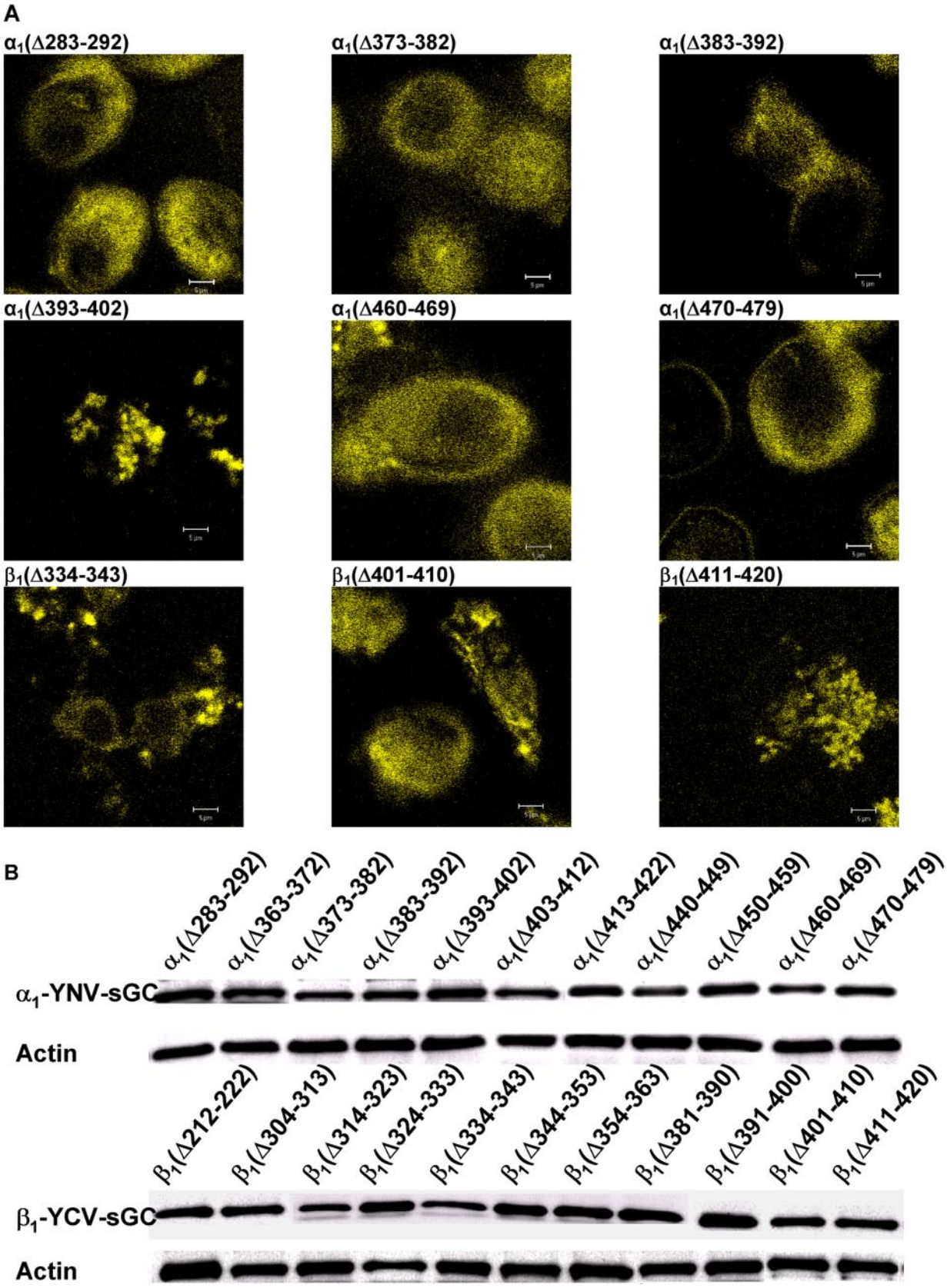

Fig. 5. Fluorescence and expression signals of sGC deletion mutants. A, fluorescence signal of representative cGMP reporter cells transiently transfected and imaged by confocal microscopy. B, Western blots of the cytosolic fractions of cGMP reporter cells transiently transfected with the indicated deletion mutants and actin, which were detected as described under *Materials and Methods*.

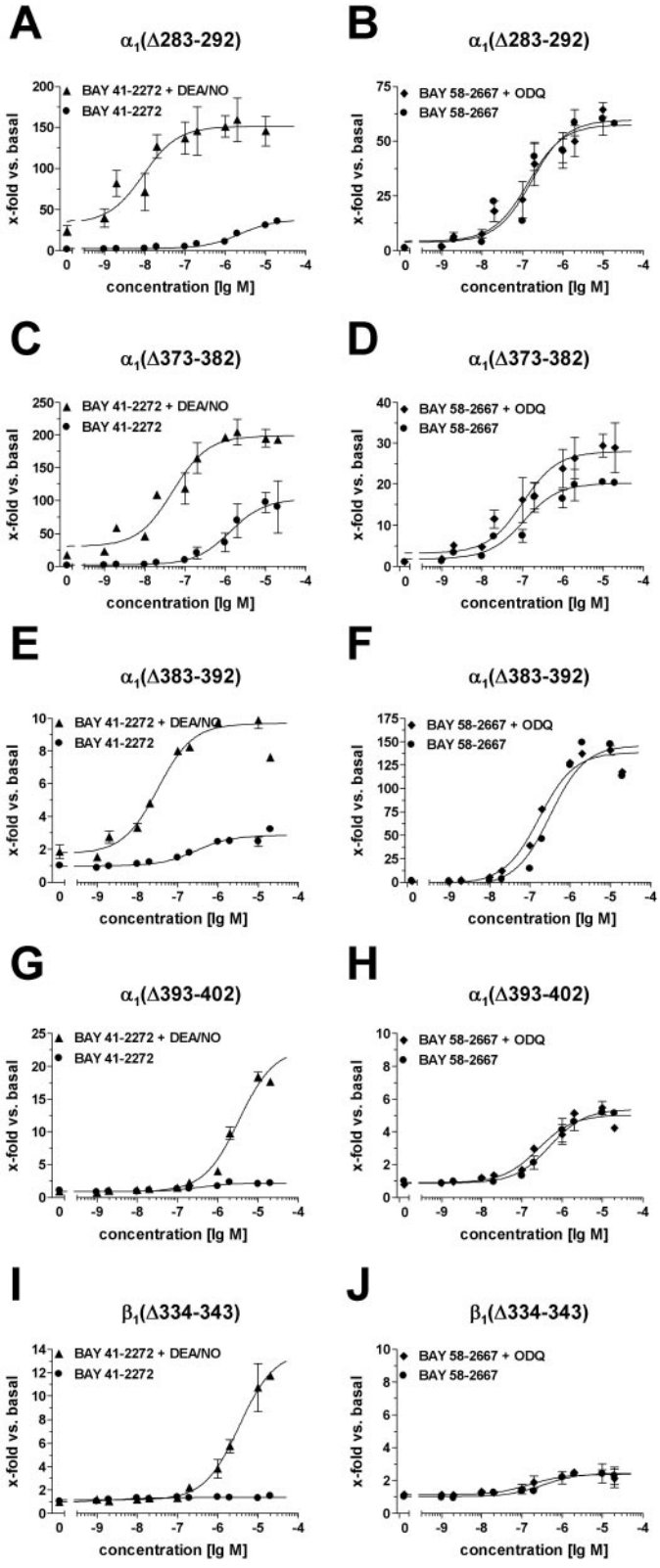

Fig. 6. Activation profile of sGC deletion mutants. Activation pattern of the indicated YFP-sGC constructs incubated with increasing concentrations of BAY 41-2272 or BAY 58-2667 alone or in the presence of a fixed concentration DEA/NO (10 nM) or ODQ (10 μM), respectively. cGMP reporter cells were transiently cotransfected with the α_1- and β_1-subunit of sGC. Enzyme activation is represented as -fold compared with the transfected but not stimulated control. Data are shown as mean ± S.E.M. from three to five independent experiments performed in quadruplicate.

bound guanylate cyclase A (GC-A) and supported later by studies showing that a construct encoding residues 1–385 of β_1-sGC is capable of forming homodimers (Wilson and Chinkers, 1995; Zhao and Marletta, 1997). Subsequent coprecipitation analyses of truncated and/or mutated sGC indicated that segments spanning $\alpha_1$61–128, $\alpha_1$367–462, $\alpha_1$421–454, $\beta_1$204–244, and $\beta_1$379–408 contribute to α_1/β_1-heterodimerization (Zhou et al., 2004; Shiga and Suzuki, 2005; Wagner et al., 2005).

In the present analysis, we validated and refined published sequences and tried to identify novel residues involved in α_1/β_1-sGC heterodimerization. In contrast to published work, we monitored the formation of sGC α_1/β_1-heterodimers and their activation profile in living cells by a unique combination of the BiFC approach and a cGMP reporter cell line (Hu et al., 2002; Schmidt et al., 2004; Wunder et al., 2005; Kerppola 2006a,b; Rothkegel et al., 2006).

The generally accepted fact that both subunits have developed from a common ancestor and published results showing that sGC α- and β-subunits are capable of forming homodimers and heterodimers suggested the existence of a conserved homologous dimerization motif in both subunits of the enzyme (Zhao and Marletta, 1997; Zabel et al., 1999; Iyer et al., 2003). Therefore, we constructed a sequence alignment to identify conserved segments within the predicted dimerization regions of α_1/β_1-sGC (Fig. 4). These identified segments were systematically deleted, and the generated deletion mutants characterized by transient transfection into the cGMP reporter cell line. The screen of the heterodimerization profile of the deletion mutants by BiFC revealed that coexpression of the deletion mutants $\alpha_1$283–292, $\alpha_1$373–382, $\alpha_1$383–392, $\alpha_1$393–402, $\alpha_1$460–469, and $\alpha_1$470–479 with β_1-sGC and $\beta_1$334–343, $\beta_1$401–410, and $\beta_1$411–420 with α_1-sGC resulted in a fluorescence similar to native α_1/β_1-sGC, indicating that these deletion mutants were still able to dimerize. Thus, the deleted amino acid regions are not involved in α_1/β_1-sGC heterodimerization (Fig. 4, green/yellow shaded segments). Of the deletion mutants listed above that showed fluorescence, $\alpha_1$283–292, $\alpha_1$373–382, $\alpha_1$383–392, $\alpha_1$393–402, and $\beta_1$334–343 showed enzymatic activity, thus corroborating the results obtained from the BiFC assay. Although some of these deletions ($\alpha_1$283–292, $\alpha_1$373–382, $\alpha_1$393–402, and $\beta_1$334–343) resulted in measurable alterations of the BAY 41-2272 and/or DEA/NO activation profile, the presence of catalytic activity in combination with the observed fluorescence indicated clearly the formation of functional heterodimers. These observed alterations of sGC activation as well as the loss of any enzymatic activity in the case of the fluorescent deletion mutants $\alpha_1$460–469, $\alpha_1$470–479, $\beta_1$401–410, and $\beta_1$411–420 suggest that although these residues might not be critical for sGC dimerization, the mutations directly disturbed or even impaired the mechanism of enzyme activation.

All fluorescent mutants, except for the deletion constructs $\alpha_1$393–402, $\beta_1$334–343, and $\beta_1$411–420, showed a homogenous localization in the cytosol. Although Western blot analysis revealed no significant changes in the expression levels of any generated mutant, these three deletion mutants showed a more inhomogeneous distribution. This difference might point to deletion-induced problems with regard to proper protein folding that could result in the aggregation of misfolded proteins and, in turn, lead to unspecific BiFC sig-

nals (Ozalp et al., 2005). However, $\alpha_1$393–402 and $\beta_1$334–343 were enzymatically active, indicating the formation of functional sGC heterodimers. Whether this cGMP formation was catalyzed by potentially aggregated sGC or by a small subpopulation of correctly folded enzyme in the cytosol remains an open question, because the cGMP reporter cell does not provide spatial information about the cGMP synthesis as FRET-based methods do (Honda et al., 2001; Nikolaev et al., 2006). Nevertheless, the observed catalytic activity indicates the formation of functional sGC, ruling out an involvement of these residues in the process of heterodimerization.

Deletion of amino acid regions $\alpha_1$363–372, $\alpha_1$403–412, $\alpha_1$413–422, $\alpha_1$440–449, $\alpha_1$450–459 and $\beta_1$212–222, $\beta_1$304–313, $\beta_1$314–323, $\beta_1$324–333, $\beta_1$344–353, $\beta_1$354–363, $\beta_1$381–390, and $\beta_1$391–400 caused loss of fluorescence and of enzymatic activity. Because the corresponding Western blots showed unaltered expression levels of the constructed mutant enzymes, these results strongly suggest an involvement of these segments in α_1/β_1-sGC heterodimerization (Fig. 4, orange shaded segments)

Regarding the sGC β_1-subunit, it has been reported that amino acids $\beta_1$204–408 mediate sGC heterodimerization (Zhou et al., 2004). A more detailed analysis of this region identified two separate contact interfaces of β_1-sGC with α_1-sGC: an N-terminal binding site (NBS) segment consisting of amino acids $\beta_1$204–244 and a C-terminal binding site (CBS) region consisting of amino acids $\beta_1$379–408 (Zhou et al., 2004). In addition, Shiga and Suzuki (2005) hypothesized that a putative amphipathic α-helix region formed by the region $\beta_1$367–395 of rat-sGC mediates β_1-subunit dimerization with α_1-sGC (Shiga and Suzuki, 2005). In good agreement with published data, the present BiFC analysis revealed that the segments $\beta_1$212–222, $\beta_1$304–333, $\beta_1$344–363, and $\beta_1$381–400 are involved in heterodimerization with α_1-sGC, thus confirming the importance of the identified NBS and CBS segments and, at least in part, the involvement of the predicted amphipathic helix region in sGC subunit dimerization. Furthermore, the present study goes further, showing that, in addition to the NBS, CBS, and the α-helix contact interfaces, amino acid segments $\beta_1$304–333 and $\beta_1$344–363 play a critical role in sGC heterodimerization. The contribution of these amino acid segments that is partially in agreement with the very early pGC-homology-based prediction of the dimerization region was not identified by the previous coprecipitation studies, probably because of the methodological limitations of this approach.

Concerning the sGC α_1-subunit, mutagenic and coprecipitation studies revealed that mainly the central region ($\alpha_1$367–467) of α_1-sGC mediates the heterodimerization with the corresponding β_1-subunit (Shiga and Suzuki, 2005; Wagner et al., 2005). Based on the known homologies (Iyer et al., 2003), it was further hypothesized that the α_1-dimerization region consists of a discontinuous binding motif as already observed for the sGC β_1-subunit, namely an NBS-like region ($\alpha_1$271–312) and a CBS-like region ($\alpha_1$438–467; Zhou et al., 2004). In addition, structure prediction algorithms lead to the conclusion that the sGC α_1-subunit may contain an amphipathic helical binding motif ($\alpha_1$421–454) as postulated for the sGC β_1-subunit (Shiga and Suzuki, 2005; Cary et al., 2006). Further studies by site-directed mutagenesis, especially of conserved leucines within the predicted α-helix, revealed that, indeed, mainly the amphipathicity of this secondary structure seems to be crucial for sGC dimerization (Shiga and Suzuki, 2005).

By using the BiFC approach, we were able to validate and refine these findings. From the predicted region, mainly the amino acids segments $\alpha_1$363–372, $\alpha_1$403–422, and $\alpha_1$440–459 contribute to sGC dimerization, suggesting a discontinuous make-up of the α_1/β_1-sGC contact interface. In contrast to the importance of the β_1NBS and in good agreement with the analysis of the dimerization region of the medaka fish α_1-sGC, the BiFC approach detected no contribution of the putative α_1NBS to sGC dimerization (Shiga and Suzuki, 2005). However, in contrast to the work of Shiga and Suzuki (2005), our deletion mutant ($\alpha_1$283–292) showed enzymatic activity. This discrepancy might be explained by the fact that Shiga and Suzuki (2005) investigated a heavily truncated deletion mutant ($\alpha_1\Delta$1–312), which could lead to misfolding and, as a consequence, result in the expression of nonfunctional sGC.

Whereas the α_1NBS seems to have no impact on sGC dimerization, our BiFC approach showed that deletions of $\alpha_1$440–449 and $\alpha_1$450–459 within the postulated α_1CBS-like site ($\alpha_1$438–467) and the predicted amphipathic α-helix ($\alpha_1$421–454) abolished subunit dimerization and, as a result, any enzymatic activity. This observation is in good agreement with published work, thus confirming the importance of the α_1CBS and, in addition, the impact of the conserved leucines within the amphipathic α-helix for sGC dimerization (Shiga and Suzuki, 2005). Moreover, in addition to the above-discussed CBS and amphipathic α-helical region, the BiFC approach revealed that the amino acid regions $\alpha_1$363–372 and $\alpha_1$403–422 are critical α_1/β_1-sGC heterodimerization.

One coprecipitation study using bovine sGC reported that the N-terminal amino acids $\alpha_1$61–128 mediate heterodimerization (Wagner et al., 2005). However, this sequence is not conserved, and the same study showed, in good agreement with previous data, that basal activity of further deletion mutants of the N-terminal α_1-subunitis was preserved (Wedel et al., 1995; Wagner et al., 2005). Furthermore, the recently reported analysis of the dimerization region of medaka fish α_1-sGC showed, in good agreement with a previous study of the human sGC, that deletion of the α_1-sGC N-terminal 280 amino acids has no consequence for the activation profile of sGC, thus supporting the idea that amino acids $\alpha_1$61–128 are not involved in sGC heterodimerization (Koglin and Behrends, 2003; Shiga and Suzuki, 2005).

In conclusion, the present study identified the involvement of amino acid segments $\alpha_1$363–372, $\alpha_1$403–422, $\alpha_1$440–459, $\beta_1$212–222, $\beta_1$304–333, $\beta_1$344–363, and $\beta_1$381–400 in α_1/β_1-sGC heterodimerization, thus supporting the assumption that α_1/β_1-sGC heterodimerization is mediated via a discontinuous binding module (Fig. 4). Moreover, the results of our characterization of amino acid segments critical for α_1/β_1-sGC dimerization in native cells support the prediction that mainly the central regions of α_1- and β_1-sGC containing an amphipathic α-helix structure are required for the formation of a functionally active α_1/β_1-sGC heterodimer. In addition, we could herewith demonstrate that the BiFC method, in combination with a cGMP readout cell line and the recently discovered modulators of sGC activity, represents a powerful tool to further elucidate the process of sGC subunit dimerization and sGC activation. However, final clarification of the contribution of single amino acids to the process of dimeriza-

tion is dependent on the resolution of the crystal structure of native sGC.

Acknowledgments

We are grateful to Dr. Tom Kerppola (University of Michigan, Ann Arbor, MI) for providing the BiFC vectors. We also thank Yvonne Keim and Anna Kebig for outstanding technical assistance.

References

Alonso-Alija C, Heil M, Flubacher D, Naab P, Stasch JP, Wunder F, Dembowsky K, Perzborn E, and Stahl E (2001), inventors; Bayer AG, assignee. Novel derivatives of dicarboxylic acid having pharmaceutical properties. World Patent no. WO0119780. 2001 March 22

Becker EM, Wunder F, Kast R, Robyr C, Hoenicka M, Gerzer R, Schröder H, and Stasch JP (1999) Generation and characterization of a stable soluble guanylate cyclase-overexpressing CHO cell line. *Nitric Oxide* **3:**55–66.

Bender AT and Beavo JA (2006) Cyclic nucleotide phosphodiesterases: molecular regulation to clinical use. *Pharmacol Rev* **58:**488–520.

Cary SPL, Winger JA, Derbyshire ER, and Marletta MA (2006) Nitric oxide signaling: no longer simply on or off. *Trends Biochem Sci* **31:**231–239.

Evgenov OE, Pacher P, Schmidt PM, Haskó G, Schmidt HH, and Stasch JP (2006) NO-independent stimulators and activators of soluble guanylate cyclase: discovery and therapeutic potential. *Nat Rev Drug Discov* **5:**755–768.

Feil R and Kemp-Harper B (2006) cGMP signalling: from bench to bedside. Conference on cGMP generators, effectors and therapeutic implications. *EMBO Rep* **7:**149–153.

Gerzer R, Hofmann F, and Schultz G (1981) Purification of a soluble, sodium-nitroprusside-stimulated guanylate cyclase from bovine lung. *Eur J Biochem* **116:**479–486.

Gladwin MT (2006) Deconstructing endothelial dysfunction: soluble guanylyl cyclase oxidation and the NO resistance syndrome. *J Clin Invest* **9:**2330–2332.

Harteneck C, Koesling D, Söling A, Schultz G, and Bohme E (1990) Expression of soluble guanylyl cyclase. Catalytic activity requires two enzyme subunits. *FEBS Lett* **272:**221–223.

Hobbs AJ (2002) Soluble guanylate cyclase: an old therapeutic target re-visited. *Br J Pharmacol* **136:**637–640.

Hoenicka M, Becker EM, Apeler H, Sirichoke T, Schröder H, Gerzer R, and Stasch JP (1999) Purified soluble guanylyl cyclase expressed in a baculovirus/Sf9 system: stimulation by YC-1, nitric oxide, and carbon monoxide. *J Mol Med* **77:**14–23.

Honda A, Adams SR, Sawyer CL, Lev-Ram V, Tsien RY, and Dostmann WR (2001) Spatiotemporal dynamics of guanosine 3′,5′-cyclic monophosphate revealed by a genetically encoded, fluorescent indicator. *Proc Natl Acad Sci U S A* **98:**2437–2442.

Hu CD, Chinenov Y, and Kerppola TK (2002) Visualization of interaction among bZip and Rel familiy proteins in living cells using bimolecular fluorescence complementation. *Mol Cell* **9:**789–798.

Iyer LM, Anantharaman V, and Aravind L (2003) Ancient conserved domains shared by animal soluble guanylyl cyclases and bacterial signaling proteins. *BMC Genomics* **4:**5.

Kerppola TK (2006a) Complementary methods for studies of protein interactions in living cells. *Nat Methods* **3:**969–971.

Kerppola TK (2006b) Visualization of molecular interactions by fluorescence complementation. *Nat Rev Mol Cell Biol* **7:**449–456.

Koglin M and Behrends S (2003) A functional domain of the α_1 subunit of soluble guanylyl cyclase is necessary for activation of the enzyme by nitric oxide and YC-1 but is not involved in heme binding. *J Biol Chem* **278:**12590–12597.

Luttrell LM (2006) Transmembrane signaling by G-protein-coupled receptors. *Methods Mol Biol* **332:**3–49.

Mergia E, Russwurm M, Zoidl G, and Koesling D (2003) Major occurrence of the new alpha2beta1 isoform of NO-sensitive guanylyl cyclase in brain. *Cell Signal* **15:**189–195.

Nighorn A, Byrnes KA, and Morton DB (1999) Identification and characterization of a novel beta subunit of soluble guanylate cyclase that is active in the absence of a second subunit and is relatively insensitive to nitric oxide. *J Biol Chem* **274:**2525–2531.

Nikolaev VO, Gambaryan S, and Lohse MJ (2006) Fluorescent sensors for rapid monitoring of intracellular cGMP. *Nat Methods* **3:**23–25.

Nioche P, Berka V, Vipond J, Minton N, Tsai AL, and Raman CS (2004) Femtomolar sensitivity of a NO sensor from Clostridium botulinum. *Science* **306:**1550–1553.

Ozalp C, Szczesna-Skorupa E, and Kemper B (2005) Bimolecular fluorescence complementation analysis of cytochrome P450 2C2, 2E1, and NAPDH-cytochrome P450 reductase molecular interactions in living cells. *Drug Metab Dispos* **33:**1382–1390.

Pellicena P, Karow DS, Boon ES, Marletta MA, and Kuriyan J (2004) Crystal structure of an oxygen-binding heme domain related to soluble guanylate cyclases. *Proc Natl Acad Sci U S A* **101:**12854–12859.

Rothkegel C, Schmidt PM, Stoll F, Schroder H, Schmidt HH, and Stasch JP (2006) Identification of residues crucially involved in soluble guanylate cyclase activation. *FEBS Lett* **580:**4205–4213.

Russwurm M, Behrends S, Harteneck C, and Koesling D (1998) Functional properties of a naturally occuring isoform of soluble guanylyl cyclase. *Biochem J* **335:**125–130.

Schmidt PM, Rothkegel C, Wunder F, Schröder H, and Stasch JP (2005) Residues stabilizing the heme moiety of the nitric oxide sensor soluble guanylate cyclase. *Eur J Pharmacol* **513:**67–74.

Schmidt PM, Schramm M, Schröder H, Wunder F, and Stasch JP (2004) Identification of residues crucially involved in the binding of the heme moiety of soluble guanylate cyclase. *J Biol Chem* **279:**3025–3032.

Shiga T and Suzuki N (2005) Amphipathic α-Helix mediates the heterodimerization of soluble guanylyl cyclase. *Zoolog Sci* **22:**735–742.

Stasch JP, Becker EM, Alonso-Alija C, Apeler H, Debowsky K, Feurer A, Gerzer R, Minuth T, Perzborn E, Pleiss U, Schroeder H, Schroeder W, Stahl E, Steinke W, Straub A, and Schramm M (2001) NO-independent regulatory site on soluble guanylate cyclase. *Nature* **410:**212–215.

Stasch JP, Schmidt PM, Nedvetsky PI, Nedvetskaya TY, Kumar HSA, Meurer S, Deile M, Taye A, Knorr A, Lapp H, Müller H, Turgay Y, Rothkegel C, Tersteegen A, Kemp-Harper B, Müller-Esterl W, and Schmidt HH (2006) Targeting the heme-oxidized nitric oxide receptor for selective vasodilatatation of diseased blood vessels. *J Clin Invest* **116:**2552–2561.

Straub A, Stasch JP, Alonso-Alija C, Benet-Buchholz J, Ducke B, Feurer A, and Fürstner C (2001) NO-independent stimulators of soluble guanylate cyclase. *Bioorg Med Chem Lett* **11:**781–784.

Wagner C, Russwurm M, Jäger R, Friebe A, and Koesling D (2005) Dimerization of nitric oxide-sensitive guanylyl cyclase requires the α_1 N terminus. *J Biol Chem* **280:**17687–17693.

Wedel B, Harteneck C, Foerster J, Friebe A, Schultz G, and Koesling D (1995) Functional domains of soluble guanylyl cyclase. *J Biol Chem* **270:**24871–24875.

Wedel B, Humbert P, Harteneck C, Foerster J, Malkewitz J, Böhme E, Schultz G, and Koesling D (1994) Mutation of His-105 in the beta 1 subunit yields a nitric oxide-insensitive form of soluble guanylyl cyclase. *Proc Natl Acad Sci U S A* **91:**2592–2596.

Wilson EM and Chinkers M (1995) Identification of sequences mediating guanylyl cyclase dimerization. *Biochemistry* **34:**4696–4701.

Wunder F, Stasch JP, Hütter J, Alonso-Alija C, Hüser J, and Lohrmann E (2005) A cell-based cGMP assay useful for ultra-high-throughput screening and identification of modulators of the NO/cGMP pathway. *Anal Biochem* **339:**104–112.

Zabel U, Häusler C, Weeger M, and Schmidt HH (1999) Homodimerization of soluble guanylyl cyclase subunits. *J Biol Chem* **274:**18149–18152.

Zabel U, Weeger M, La M, and Schmidt HH (1998) Human soluble guanylate cyclase: functional expression and revised isoenzyme family. *Biochem J* **335:**51–57.

Zhao Y and Marletta MA (1997) Localization of the heme binding region in soluble guanylate cyclase. *Biochemistry* **36:**15959–15964.

Zhao Y, Schelvis JP, Babcock GT, and Marletta MA (1998) Identification of histidine 105 in the beta1 subunit of soluble guanylate cyclase as the heme proximal ligand. *Biochemistry* **37:**4502–4509.

Zhou Z, Gross S, Roussos C, Meurer S, Müller-Esterl W, and Papapetropoulos A (2004) Structural and functional characterization of the dimerization region of soluble guanylyl cyclase. *J Biol Chem* **279:**24935–24943.

Address correspondence to: Priv.-Doz. Dr. Johannes-Peter Stasch, Bayer HealthCare, Cardiovascular Research, Aprather Weg 18a, D-42096 Wuppertal, Germany. E-mail: johannes-peter.stasch@bayerhealthcare.com